DTIC FILE COPY

(4)

A TECHNICAL REPORT

Contract No. N00014-88-K-0111

MODELING THE TEMPERATURE RISE AT THE TIP OF A FAST CRACK

Submitted to:

Office of Naval Research
800 North Quincy Street
Arlington, Virginia 22217-5000
Attention: Dr. George R. Yoder

Submitted by:

Heinz G. F. Wilsdorf
William G. Reynolds Professor of Materials Science

Report No. UVA/525425/MS89/104

August 1989

DEPARTMENT OF MATERIALS SCIENCE
UNIVERSITY OF VIRGINIA
SCHOOL OF ENGINEERING AND APPLIED SCIENCE
CHARLOTTESVILLE, VA 22903-2442

A TECHNICAL REPORT

Contract No. N00014-88-K-0111

MODELING THE TEMPERATURE RISE AT THE TIP OF A FAST CRACK

Submitted to:

Office of Naval Research
800 North Quincy Street
Arlington, Virginia 22217-5000

Attention: Dr. George R. Yoder

Submitted by:

Heinz G. F. Wilsdorf
William G. Reynolds Professor of Materials Science

DEPARTMENT OF MATERIALS SCIENCE
SCHOOL OF ENGINEERING AND APPLIED SCIENCE
UNIVERSITY OF VIRGINIA
CHARLOTTESVILLE, VA 22903-2442

Report No. UVA/525425/MS89/104

August 1989

REPORT DOCUMENTATION PAGE

Form Approved
OMB No. 0704-0188

1. AGENCY USE ONLY (*Leave blank*)	2. REPORT DATE	3. REPORT TYPE AND DATES COVERED
	August 1989	Interim [Technical]

4. TITLE AND SUBTITLE
Modeling the Temperature Rise at the Tip of a Fast Crack

5. FUNDING NUMBERS
C-N00014-88-K-0111

6. AUTHOR(S)
Kasi Jagannadham and Heinz G. F. Wilsdorf

7. PERFORMING ORGANIZATION NAME(S) AND ADDRESS(ES)
University of Virginia
Department of Materials Science

8. PERFORMING ORGANIZATION REPORT NUMBER
UVA/525425/MS89/104

9. SPONSORING/MONITORING AGENCY NAME(S) AND ADDRESS(ES)
Department of the Navy
Office of Naval Research
800 North Quincy Street
Arlington, VA 22217-5000

10. SPONSORING/MONITORING AGENCY REPORT NUMBER
-

11. SUPPLEMENTARY NOTES

12a. DISTRIBUTION/AVAILABILITY STATEMENT
Approved for public release; distribution unlimited

12b. DISTRIBUTION CODE

13. ABSTRACT (*Maximum 200 words*)

14. SUBJECT TERMS

15. NUMBER OF PAGES
52

16. PRICE CODE

17. SECURITY CLASSIFICATION OF REPORT	18. SECURITY CLASSIFICATION OF THIS PAGE	19. SECURITY CLASSIFICATION OF ABSTRACT	20. LIMITATION OF ABSTRACT
Unclassified	Unclassified		

NSN 7540-01-280-5500

Standard Form 298 (890104 Draft)
Prescribed by ANSI Std. 239-18
298-01

MODELING THE TEMPERATURE RISE

AT THE TIP OF A FAST CRACK

Kasi Jagannadham* and Heinz G. F. Wilsdorf**

*Department of Materials Science and Engineering
North Carolina State University
Raleigh, North Carolina 27695-7916

**Department of Materials Science
University of Virginia
Charlottesville, Virginia 22901

ABSTRACT

Temperature changes that take place ahead of a crack tip in the plastic zone have been analyzed using dislocation modeling of the plastic zone. The development of the process zone and that of the plastic zone is described in terms of dislocation generation and their movement at high strain rates of deformation. Among the various terms contributing to the total energy, the energy dissipation terms have been identified. In particular, the plastic work dissipation rate has been calculated using the phonon viscous drag forces acting on the dislocations. In our analysis, the transition from the heavily deformed process zone to the less heavily deformed plastic zone is gradual and continuous. The dislocation generation is considered more important than the dislocation velocity in the dissipation of plastic work at high strain rates of deformation. More importantly, the work hardening nature of plastic deformation in the plastic zone, the strain rate and the temperature dependence of the flow stress have been incorporated in the determination of dislocation generation in the plastic zone. The stress field

associated with a moving elastic crack tip is used to determine the increment of dislocation density and the rate of dissipation of plastic work. A finite difference approximation of the heat equation with the temperature dependent thermal conductivity and specific heat has been used to follow the temperature changes occurring at the crack tip. The results of numerical analysis of the temperature changes and the various terms contributing to the development of the plastic zone are presented to show the influence of several factors, namely loading rate, dislocation velocity, flow stress, and the crack tip radius. Scanning electron microscopy observations of local molten regions on the fracture surface of titanium alloys provided an experimental temperature range which was explained in terms of the present modeling.

Introduction

In the past considerable attention has been given to the formation of a plastic zone at a crack tip [1-6] and the resultant changes in temperature. Both, continuum plasticity theories [7] and those employing dislocation representation [8,9] have been used to relate the shape and size of the plastic zone, the yield stress and the crack tip stress field for a given mode of the applied stress. The fracture toughness of several materials, determined experimentally at low strain rates of deformation, have been interpreted in terms of the crack tip plastic deformation [4,6,10]. Further, experimental observations on several low strength materials at higher strain rates exhibit a reduction in fracture toughness [11,12]. A specific class of high strength materials including two titanium alloys and some high strength steels [4,13-15] exhibit an increase in fracture toughness at higher strain rates. Whereas the decrease in fracture toughness of a material is interpreted in terms of reduction in plasticity and an increase in flow stress at higher strain rates [3,4,6], the appearence of a minimum followed by an increase in fracture toughness is associated with improved plastic deformation ahead of the crack tip as a result of the temperature rise brought about by the dissipation of plastic work [4,14,16]. Thus, the study of fracture behavior of a material under fast loading conditions leading to high strain rate deformation involves an evaluation of temperature changes brought about by crack tip deformation [6,14,16]. A preliminary evaluation of the temperature rise ahead of the crack tip has shown [14,17] that the loading rate is an important factor in addition to the thermal conductivity of the region in the plastic zone associated with the crack tip. In this paper, we consider the various factors that contribute to the dissipation of plastic work in the plastic zone and evaluate the temperature changes. Specifically, the partially melted dimple walls observed in scanning electron microscopic observations of fracture surfaces[14,17] will be interpreted through two terms of plastic energy dissipation. First, the dissipation of frictional energy associated with the plastic deformation in the plastic zone will be given attention. Second, the importance of this term, in comparison to the plastic work, arising from high strain rate void growth and plastic deformation associated with ligament rupture leading to coalescence with the crack tip will be discussed. It is well known[17-21] that high strain rate fracture of ductile metals and alloys involves the nucleation and growth of voids ahead of a fast propagating crack, and the contribution of the dissipation of plastic work arising from these changes must be included in the temperature accounting.

Experimental Observations

Experimental observations on Ti-10V-2Fe-3Al under fast loading conditions have been correlated[22,23] to determine the loading rate as a function of crack growth velocity, strain rate and fracture toughness. These results may be described through the loading rate parameter, $\dot{K}$, as follows

$$\dot{K} = 968\,(V_c)^{0.387} = 900\,\dot{\varepsilon} \qquad (\text{in MPa.sec}^{-1}) \qquad (1)$$

and $$K_{Ic} = 32.6 + 6.2\,\ln(\dot{K}) \qquad (\text{in MPa}\sqrt{m}) \qquad (2)$$

where V_c is the crack growth velocity, K the loading rate parameter and K_{Ic} the fracture toughness. The presence of limited, local molten regions in the crack tip plastic zone where final ligament rupture has taken place are characterized by scanning electron micrographs as shown in Figure 1. These molten regions are seen at dimple walls on fracture surfaces where void growth and coalescence had taken place at high strain rates. Figures 2(a) and (b) illustrate the development of multiple ruptures and shear zones at the separation of microligaments, as observed during an in-situ test in the transmission electron microscope. These processes can be interpreted in terms of dislocation theory since they are taking place at a thickness of approximately one micrometer or less[24-26]. It has been shown earlier[14] that the rupture of microligaments effecting the coalescence of voids can add a temperature rise between 300°C and 500°C dependent on strain rate and local material strength.

The above relations suggest that the macroscopic strain rate of plastic deformation in the specimen increases with increasing loading rate or crack tip velocity. The strain rate as given by the Orowan equation[27],

$$\dot{\varepsilon} = \phi \rho b V \qquad (3)$$

where ϕ is a geometric factor approximately equal to unity, ρ the dislocation density, b the Burgers vector and V the dislocation velocity, shows that either the dislocation density or the dislocation velocity should increase in the plastically deformed region in order to give rise to an increase in strain rate. We will examine the significance of this result on the temperature changes ahead of the crack tip. The frictional stress against the generation and movement of dislocations in the plastic zone is higher at higher strain rates of plastic deformation and this significantly alters the resultant changes taking place at the tip[25-26].

Energy Changes Associated with a Crack

The energy changes that take place ahead of the crack tip are responsible for the temperature rise in the plastic zone and hence a clear description of the energy terms associated with the crack configuration becomes important. The work done by the applied stress in opening the crack surfaces and extending the crack is spent in the formation of plastic work to generate the plastic zone and the surface energy to create the additional crack surfaces. The strain energy released when an elastic crack extends consists of the sum of an increase in the elastic distortional energy , a positive term and the work done by the applied stress, a negative term. Thus , a net decrease in the total energy obtains if changes in the surface energy are not included. On the other hand, for a plastic crack, the elastic strain energy of distortion associated with the crack and the plastic zone are positive while the work done by the applied stress in creating the crack surfaces and the plastic zone is negative. The shear component of the applied stress and the crack tip stress field perform the work on the slip planes in the plastic zone. An additional term arises in the generation of the plastic zone which is the frictional energy dissipated in the movement of dislocations.

A better understanding of the energy changes in front of the crack tip may be obtained by a dislocation description of the crack and the plastic zone, as shown in Figure 3. Specifically, the distortion associated with the newly generated crack surfaces may be represented in terms of crack dislocations that satisfy the free surface boundary conditions. The plastic zone consists of a distribution of lattice dislocations generated in response to the shear component of the applied and the crack tip stress field. The self and interaction energy terms associated with the dislocation configuration, either representing the crack region or the plastic zone, constitute the elastic strain energy. In particular, the interaction energy between the elastic crack dislocations and the lattice dislocations in the plastic zone is the inseparable term in energy associated with the plastic crack.

The energy changes associated with a stable plastic crack may be derived from the dislocation model. It has been shown[30] in consideration of the equilibrium of the crack configuration that the following constitutive energy equations are observed.

$$\begin{aligned} E_{S_c} + E_{I_c} + E_{I_{cl}} /2 &= E_{W_c} /2 \\ E_{S_1} + E_{I_1} + E_{I_{cl}} /2 &= -(E_f - E_{w_1})/2 \end{aligned} \tag{4}$$

so that the total energy of the crack configuration is given by

$$\begin{aligned} E_T &= (E_e - E_{W_c} - E_{W_1} + E_f) + E_\gamma \\ &= -(E_{W_c} + E_{W_1} - E_f)/2 + E_\gamma \end{aligned} \tag{5}$$

In the above equation, the elastic strain energy E_e includes E_s, the self energy and E_I, the interaction energy of dislocations. Further, E_W is the work done by the applied and crack tip stress, and E_f

is the lattice frictional stress. The subscript c stands for the energy terms associated with crack dislocations, l for lattice dislocations and cl for the cross term between crack and lattice dislocations. The surface energy term E_γ arises from newly generated crack surfaces when the crack extends. It is seen from these energy terms that dissipation of energy in the form of heat does not arise from the work done, E_w. Instead, the dissipated energy arises from the frictional resistance offered by the lattice to the movement of lattice dislocations in the plastic zone, E_f . These energy terms include the velocity dependence[31] for a fast moving plastic crack. The driving force associated with the crack tip can be written as the energy gradient with respect to crack size

$$- E'_T = E'_w - E'_e + E'_f = -(E'_{w_c} + E'_{w_l} - E'_f) /2 \qquad (6)$$

The same equation applied to a dynamic crack[31] takes the form

$$-E'_T = E'_w - E'_e - E'_k - E'_f \qquad (7)$$

where E_k is a term separated out of E_e and represents the kinetic energy associated with the crack. The term E_k for moving dislocations consists of the velocity dependence of the self and interaction energy terms which cannot be separated from E_e. Thus $E_e + E_k$ consists of the total strain energy term associated with the dynamic crack configuration. The dissipated energy ahead of the crack tip in the plastic zone is responsible for the temperature changes.

Process Zone and Transition to the Plastic Zone

The crack tip region wherein plastic deformation takes place is divided into two regions as shown in Figure 4 to distinguish the severely deformed regions from those where plasticity is not very extensive. It should be pointed out that the demarcation between the two regions is not very rigid. Specifically, we may conveniently define the process zone as a region with a dislocation density greater than 10^{16} m^{-2}. Also, the process zone immediately at the tip is the region wherein the final stages of plastic deformation will occur with ligament rupture. Crack growth behavior is essentially determined by the properties of the material in the process zone[19-2)]. The nucleation of microvoids and their growth to coalescence with the crack tip occurs in the process zone as seen in the transmission electron micrograph of an in-situ deformed foil, shown in Figures 2a and 2b. The growth of the crack at higher strain rates deviates from the path along the maximum normal stress axis as a result of the void coalescence with the crack tip. The present experimental results[14-17)] further suggest considerable branching of the crack growth at very high strain rates.

We do not specifically analyze the temperature changes brought about by plastic deformation within the final ligament failure. These have been already estimated to give rise to large changes in temperature when high strain rates are involved[14,21,32)]. However, the temperature changes resulting from concentrated plastic deformation within the process zone will be determined. Furthermore, the transition from the process zone to the plastic zone is continuous and arises from a decrease in the dislocation density. Previous estimates of temperature changes brought about by adiabatic deformation by glide on several parallel slip planes[14] show that it could be as much as 300°C to 500°C. The experimental observations of molten regions at dimple walls on fracture surfaces of two titanium alloys illustrate that these regions of final ligament rupture are responsible for the high temperatures attained during high strain rate fracture. Furthermore, continuum plasticity analysis of void growth in the process zone[21] incorporating the constant mobile dislocation density shows that large strains occur during the final ligament coalescence with the crack tip. Such large strains within microseconds are expected to give rise to a near adiabatic temperature rise reaching the melting point of these titanium alloys. It is further realized that dynamic void growth at very high strain rates is essentially controlled by high rates of dislocation generation and not dislocation velocity. Thus, dynamic crack propagation under high strain rates involves both nucleation and coalescence processes of voids in the process region where low energy dislocation cell walls are readily formed. There is now ample evidence that voids are readily nucleated along these dislocation cell walls[33].

Dissipative and Non-dissipative Processes in the Plastic Zone

The movement of lattice dislocations in a crystal is subject to two types of forces, namely, dissipative and non- dissipative forces[34]. The non-dissipative forces consist of those which are not responsible for generation of heat and the energy is conserved when dislocation motion takes place. Several examples of these may be mentioned. Thus, for example elastic dislocation-dislocation interactions and dislocation-point defect interactions, Peierls force acting in the lattice, and forces associated with the curvature of the lattice dislocations are all classified as non-dissipative forces. On the other hand, drag forces arising from phonons, electrons and thermoelastic losses are included in the dissipative forces[35]. When the dissipative phonon viscous drag force predominates over all the other forces that retard the dislocation motion, a constant resolved shear stress, τ, will produce a terminal velocity, V, associated with the dislocation such that the driving force per unit length, τb, is equal to the viscous force per unit length, BV, where B is the drag coefficient. Thus

$$B = \tau b/V \tag{8}$$

The magnitude of the drag coefficient for a dislocation of known Burgers vector, b, is determined by measurement of the viscous force at a known dislocation velocity, or by measurement of energy dissipation brought about by the viscous force. However, such experiments are complicated by the fact that non-dissipative forces[34] also act on the moving dislocations. The flow stress of a crystal is in general a fair measure of the effective non-dissipative forces. Therefore, a definitive calculation of the plastic work term using the flow stress to determine the dissipated plastic energy seems inappropriate[6,35]. A large part of the irreversible plastic work term is considered to be dissipated as heat in the lattice. The energy dissipated is also considered to be insensitive to the magnitude of the drag coefficient at low to moderate strain rates because B does not significantly influence the stress level required to maintain the deformation rate. Dislocations responsible for the plastic strain rate do not continue to accelerate after the breakaway from obstacles because of the viscous drag force. Instead, a drag limited dislocation velocity is reached after moving a few atomic distances[37)]. In order to account for the relativistic effects at high strain rates, the drag coefficient is assumed in the form,

$$B = B_o/(1-V^2/C_s^2)^{1/2} \tag{9}$$

where B_o is the drag coefficient at rest and C_s the shear wave velocity in the medium. The force required to overcome the viscous drag force by the dislocation is thus given by

$$F(Drag) = \tau b = B_o\, V/(1-V^2/C_s^2)^{1/2} \tag{10}$$

It is now important to point out that F(Drag) given by the above equation is responsible for the dissipated energy and that it is different from the flow stress in the region of the plastic zone. The temperature dependence of the drag coefficient is very important in the determination of the temperature changes that are occurring ahead of the crack tip. The phonon viscous drag force depends primarily on the phonon density or thermal energy. Therefore, the drag coefficient is expected to increase linearly with temperature at higher temperatures [35,38-40)]. The present analysis of the changes at the crack tip are made after incorporating the temperature dependence of B_o in the form,

$$B_o = 3kT/10\, C_s b^2 \tag{11}$$

where k is the Boltzmann constant.

Importance of Dislocation Generation Vs. Dislocation Motion in High Strain Rate Deformation

Several models representing plastic deformation at high strain rates[41,42] employed complete dislocations or dislocation segments in edge orientation moving at high velocities, close to transonic or supersonic velocities. The Orowan equation (3) for the plastic strain rate, $\dot{\varepsilon}$, can be used to relate various quantities so that higher strain rates are obtained at higher dislocation velocities. However, one has to realize from experimental measurements of dislocation densities[43-46] that very high dislocation generation and not high dislocation velocities are responsible for high strain rates. Also it was realized very early in the development of dislocation theory[47] that for high strain rates of deformation including the viscous drag regimes of dislocation motion, dislocation velocities are not the rate limiting factor in the strain rate deformation, but that instead the dislocation generation rate is the controlling factor. The explicit velocity dependence of the strain rate can be removed by noting that if λ is the life time of a dislocation and $\dot{\rho}$ is the rate of dislocation generation, the total mobile dislocation density ρ_m can be written as,

$$\rho_m = \dot{\rho}\tau = \dot{\rho}d/V \tag{12}$$

where d is the average distance moved by the dislocation and substitution of ρ_m from the above into the Orowan equation gives,

$$\dot{\varepsilon} = \dot{\rho}\ bd \tag{13}$$

It is seen from the above equation that the strain rate is a function of the dislocation generation rate and d is the average distance moved by the dislocation, which is assumed here to be the average distance between dislocations in a crystal. Of course, d is a function of dislocation velocity at low values but it is the average distance between dislocations at higher strain rates, i.e a function of dislocation density. The present calculations use the dislocation generation rate at the crack tip to determine the dissipated plastic work rate. Equations (3) and (13) are considered equivalent in the present analysis.

Work Hardening in the Plastic Zone

The propagation of a crack into its own plastic zone is fundamental to the consideration of the work hardening that takes place prior to the separation of material[48]. The nature of the flow stress as function of strain, strain rate and temperature should be incorporated into the development of the plastic zone ahead of the crack tip. The calculation of temperature changes involves the dislocation generation rate and not the plastic strain itself, although these two parameters are related as mentioned before. Therefore, we shall make use of the general equations of flow stress in terms of the dislocation density[49] in the form

$$\sigma = \sigma_o + \alpha G b \rho^{1/2} \tag{14}$$

where σ is the resolved component of shear stress arising from the crack tip stress field and the applied stress, σ_o the lattice frictional stress, α a constant equal to 0.5, and G is the shear modulus. This equation has been established generally by experiment and is applicable in many metals and alloys[50]. The parameter σ_o includes both the dissipative and non-dissipative forces which increase almost logarithmically with strain rate. There is a transition in the slope of the strain rate dependence of flow stress when strain rates of the order of 10^2 sec^{-1} are approached. These high strain rates are applicable in the final stages of ligament fracture in the process zone. However, the material prior to final fracture deforms at much lower strain rates below this transition. A linear increase of frictional stress with the logarithm of strain rate is included in the present analysis as discussed subsequently. The dislocation density ahead of the crack tip is obtained from equation (14) for any position of the crack tip. The lowering of the frictional stress at higher temperatures with a corresponding increase in dislocation density is incorporated through the temperature dependence of the shear modulus and the lattice frictional stress in equation (14). It should be noted that dislocation annihilation and regrouping takes place simultaneously in the plastic zone at higher temperatures and it is the resultant dislocation density that is responsible for the flow stress given in equation (14).

Analysis of Changes in Various Quantities at the Crack Tip

An evaluation of the various quantities associated with the development of the plastic work dissipation rate responsible for temperature changes in the plastic zone is presented in this section. We make use of the stress field expressions associated with a dynamic crack as derived by Broberg[51,52] using linear elasticity. In particular, the stress on the y=0 plane of a tensile mode I crack is given by

$$\sigma_{yy} = \sigma_a \{C_s \ t/2r\}^{1/2} F(V_c) \tag{15}$$

where σ_a is the applied stress, r the distance from the crack tip and t the time from the start. The quantity C_s is the shear wave velocity and $F(V_c)$ is a function of the crack tip velocity, the shear wave velocity and the dilatational wave velocity in the medium. A detailed expression for $F(V_c)$ is found elsewhere[51,52]. We shall make use of equation (15) to represent the experimentally observed relation between crack tip velocity, V_c, and the loading rate, $\dot{K}$. The stress acting on the crack is incremented by Δt starting with an initial time, t(init) so that

$$\sigma_a = \sigma(t) = \dot{K}\{ t(init) + n \Delta t\} \qquad (16)$$

where n represents the number of increments of stress applied to the system. After each increment of time, the stress field ahead of the tip is determined as a function of the distance from the tip. The region on the plane of the crack is divided into several intervals of distance, each of size $\Delta x = V_c \Delta t$ and the stress at each point determined from equation (15). The dislocation velocity ahead of the crack tip is an important parameter[39] determined by

$$V = (\sigma_a - \sigma_o) \beta C_s/G \qquad (17)$$

where the parameter β is varied to represent the changes arising from different crack tip velocities. We believe that the dislocation velocity at the crack tip should be higher for higher crack tip velocities thereby representing higher strain rates encountered at higher loading rates as given by equations (1) and (2). Through a variation of the parameter β, it becomes possible to understand the effects of higher strain rates present at the crack tip process zone. The drag force acting on dislocations is a function of the velocity and hence it changes with the position in the plastic zone. The distance traveled by dislocations in the plastic zone is equal to the average distance between dislocations unless the dislocation velocity is low. We believe that for high loading rates considered to give rise to local molten zones, the latter is not true so that the distance traveled by the dislocation is given by $d = \rho^{-1/2}$. The plastic work dissipation rate can now be written in the form

$$\dot{W} = \tau b \rho V = F(\text{Drag}) \rho V = F(\text{Drag}) \rho d/\Delta t \qquad (18)$$

Further, we have assumed that all the dislocations present ahead of the crack tip become dynamic and thus contribute to the plastic work dissipation. The quantity $\dot{W}$ is determined as a function of the position from the crack tip for every increment of time, Δt. Thus, the region around the crack consists of a one-dimensional grid of points at which the work rate, $\dot{W}$, is determined in increments of time. The resultant temperature rise is obtained from a numerical solution of the one-dimensional heat equation[53] in the form

$$\partial T/\partial t = (K/DC)\, \partial^2 T/\partial x^2 + \dot{W}/(DC) = a \partial^2 T/\partial x^2 + \dot{W}/(DC) \qquad (19)$$

where $a=K/DC$ is the thermal diffusivity and $T(x,t)$ the temperature in the medium. In the above equation, the parameters K and C signify the thermal conductivity and the specific heat respectively whereas D represents the density of the medium. An analytical solution to the heat equation, taking the temperature dependence of the various quantities into account, is difficult to obtain so that a finite difference approximation is considered appropriate[54].

Temperature and Strain Rate Dependence of Various Quantities in the Analysis

The thermal conductivity, K and the specific heat, C, are found to increase almost linearly with temperature[55] in this alloy so that we can approximate the variation of the two quantities in the form,

$$K = 10.9\ (1+0.6\ T/1200)\ \ W/m\ ^\circ C$$
$$C = 4.9 X 10^2 (1+0.6\ T/1200)\ J/Kg\ ^\circ C \qquad (20)$$
for $0 < T < 1200$.

The temperature dependence of the shear moduli and the frictional stress[55] against movement of dislocations is given by,

$$G\ (T) = G(0)\ (1-0.5\ T/1200)\ \text{for}\ 0<T<1200 \qquad (21)$$
$$\sigma_o(T) = \sigma_o^o(1-0.25\ T/350\ )\ \text{for}\ 0<T<350$$
$$\sigma_o(T) = \sigma_o^o(0.75\ -0.5\ T/1200)\ \text{for}\ 350<T<1200 \qquad (22)$$

On the other hand, the 0.2% flow stress, σ_y, increases with strain rate in the form

$$\sigma_y(0) = 1300 + 21.8\ \ln \dot{\varepsilon} \qquad \text{(in MPa)} \qquad (23)$$

The various quantities included in the analysis are evaluated at each point of a one-dimensional grid of points at the end of every increment of time, Δt, in order to take into account the temperature and strain rate dependence. The crack tip advances by a distance of $V_c \cdot \Delta t$ so that the position of the crack tip changes from one point to the next in the grid. The stress field of the crack to the region left of the tip is below the frictional stress so that no plastic work is dissipated.

Finite Difference Approximation of the Heat Equation

The heat equation in the presence of the terms giving rise to sources of heat has been solved[6] by treating the plastic zone as a continuous distribution of sources of heat and using a linear superposition over the plastically deformed region[53]. We provide a numerical solution using a finite difference approximation in the form

$$\{T(i,j+1)-T(i,j)\}/\ \Delta t = a\ \ \{T(i+1,j)-2T(i,j)+T(i-1,j)\}/h^2 + \dot{W}(i,j+1)/DC \qquad (24)$$

with the boundary conditions in the form

$$T(1,j) = T(2,j)$$
$$T(N-1,j) = T(N,j) \tag{25}$$

where N is the total number of grid points, $h=V_c\ \Delta t$ and all other terms as defined earlier. The above boundary conditions imply that far away from the crack tip, on either side, the temperature gradients are vanishing. The first subscript, i indicates the position in units of h and the second, j refers to the time interval in units of Δt. The choice of time interval and the grid spacing, h, should be such that the stability condition[54)] is satisfied in the form

$$T(i,j-1)[1 - 2a\Delta t/h^2] + \dot{W}(i,j)\ \Delta t/DC > 0$$

The numerical computations are carried out with the following chosen values of the constants[55, 56)] applicable to the Ti- 10V-2Fe-3Al alloy. The Burgers vector of the dislocations is chosen to be 0.286 nm with the shear modulus G(0) = 41.7 GPa and Poisson's ratio, ν =0.32. The density is D=4.65 gm/cm^3 and the specific heat C=490 J/Kg °C. The interval of time Δt has been chosen between 0.25X10^{-4} to 1.0X10^{-4} depending on the crack tip velocity, with lower increments of time found better for higher values of V_c.

Results of Numerical Analysis

The changes in the temperature and other quantities that take place in the plastic zone are shown in Figures 5a to 5g as a function of position from the initial point of crack propagation. A crack nucleated at a point is allowed to grow with a constant velocity V_c associated with the tip. The applied stress acting on the crack is determined from the loading rate parameter $\dot{K}$ given by equation (1) as a function of the loading time. We have chosen three values for the crack tip velocity, $\dot{V}_c$ equal to 0.4, 0.8 and 1.6 m/sec with the corresponding loading rates given by 680, 888 and 1160 MPa/sec respectively. The stress field ahead of the crack tip rises gradually with increasing time with the crack moving elastically in a brittle manner in the initial stages. Eventually, when the stress field associated with the tip overcomes the lattice frictional stress, dislocations are generated giving rise to the dissipation in accordance with the plastic work term. The variation of the crack tip stress field in the plastic zone is shown in Figure 5a and the strain rate dependent lattice frictional stress in Figure 5b. The changes in dislocation density and the development of the plastic zone , the plastic work rate, the dislocation velocity, the plastic strain ahead of the tip and the temperature in the plastic zone are shown in Figures 4b to 4g respectively for increasing values of loading time. It is clear that the dislocation density reaches a maximum at the tip and falls rapidly with the position from the tip. The nature of variation of other quantities is similar.

We have used a value for $\delta = 0.5 V_c \Delta t$ within which the elastic stress field expressions are not valid and hence all the quantities are evaluated at positions greater than δ. The position of the tip moves for every increment of time, Δt, and hence the position of the maximum value of each quantity shown in Figures 5a to 5g also shifts with the crack tip. The temperature ahead of the crack tip increases with creation of additional plastic work but the conduction of heat reduces the temperature at the position of the crack tip corresponding to the previous increment of time. The discrete data points obtained from the finite difference approximation should be smoothened in order to represent the continuous propagation of the crack and the resultant changes ahead of the tip. The results shown in Figures 5a to 5g are obtained by this procedure. Since the conductivity and specific heat increase with increasing temperature, the width of the plastic zone also increases with time. It is seen, from equation (15), that the crack tip stress field increases with loading time, t, for a given distance from the tip. Therefore, the dislocation velocity given by equation (17), V, and the drag force given by equations (10) and (11) also increase, resulting in a higher rate of plastic work dissipated, $\dot{W}$, as given by equation (18). The net result is to increase the temperature ahead of the crack tip with increasing loading time, t. These calculations illustrate that the temperatures within the plastic zone can reach large values close to the crack tip. This region of the crack tip wherein large changes in dislocation density and plastic strain take place to give rise to a large increase in temperature corresponds to the process zone. Void nucleation in this region and void growth at high strain rates can lead to ligament rupture and further increase in temperature so that the melting temperature can be reached or exceeded locally. The failure of the specimen at a certain crack length beyond which no further increment of load is necessary for crack propagation determines the terminal point at which the melt phenomenon develops.

Influence of crack tip velocity or loading rate parameter

We present the changes in the various quantities that take place ahead of the crack tip for three values of the loading rate parameter and correspondingly three values of crack tip velocity. However, the dislocation velocity in the plastic zone is also changed by the same factor since the strain rate of deformation increases with loading rate, as found experimentally, in this alloy. In particular, the following values are chosen:

$\dot{K}$ =680 MPa /sec, V_c=0.4 meter/sec, β =10.0
$\dot{K}$ =888 MPa /sec, V_c=0.8 meter/sec, β =20.0
$\dot{K}$ =1160 MPa /sec, V_c=1.6 meter/sec, β =40.0

In all three situations, the initial position of the crack tip remains the same. Thus, for a given time of loading, a crack with a higher loading rate parameter $\dot{K}$, propagates to a larger size in the specimen. The results of the various quantities for the three different situations are shown in Figure 6. It is seen that the softening arising from the dissipation of plastic work at the crack tip has a major influence on the various quantities. Crack growth into the plastic zone is generating a higher dislocation density, and hence the plastic work dissipation rate is more effective at comparatively slower growth rates. This leads to a build-up of a higher temperature in the plastic zone. These results are to be discussed for the same time period for which loading is applied, as shown in Figure 6.

The temperature rise ahead of the crack tip at any point in the process zone arises from two factors. Firstly, the heat conducted from the higher temperature attained at a previous position of the tip leads to an increase in temperature. The temperature rise from this factor decreases with increasing crack velocity, V_c, since the crack tip is moving faster than the rate of heat conduction. Secondly, the rise in temperature arises from the plastic work dissipated which is a function of dislocation velocity, dislocation density and drag force. The build up of temperature from the second factor is not proportional at higher crack velocities if the dislocation velocity in the plastic zone increases proportionally. At the same time, a higher crack growth velocity is also responsible for a higher strain rate of deformation at which the lattice frictional stress becomes higher in the lattice. The net result is a decrease in dislocation density and the width of the plastic zone. The crack size at which it becomes unstable leading to failure of the specimen is reached earlier and hence the temperature rise is not sufficiently high in the process zone. Therefore, the local melting phenomenon cannot be observed at very high strain rates. On the other hand, the total loading time to reach the same crack size at comparatively lower crack velocity is higher with a higher rate of build up of temperature in the process zone. Assuming that the temperature rise during final ligament rupture around voids is almost the same, larger areas of molten dimple walls should be seen on the fractured surface. These results are also substantiated by the recent scanning electron microscopy observations of the fracture surface from specimens fractured during different loading rates[57)]. It should also be pointed out that when the crack velocity reaches a lower limit, the rate of heat dissipation becomes faster than the rate of generation ahead of the crack tip. This factor depends on the temperature dependent thermal conductivity and the specific heat which increase with temperature. The plastic work dissipation rate also becomes lower at lower crack velocities. Thus we expect a certain critical loading rate and crack growth velocity for which the temperature rise will be highest in the plastic zone and therefore molten regions of highest areal density should be observed in the scanning electron micrographs.

We shall now present the results of increasing the loading rate and crack tip velocity without increasing the dislocation velocity in the plastic zone. This is a hypothetical situation wherein the higher macroscopic strain rates in the specimen responsible for higher loading rates may be obtained, without higher dislocation velocities in the process zone. Thus, we separate the crack tip process zone from the remaining part of the specimen and consider the dislocation velocity to be stress dependent only. This is assumed to be a microstructural dependent deformation behavior wherein higher mobile dislocation densities are attained in the process zone without altering the dislocation velocity. It is important to clearly distinguish the strain rates at the crack tip process zone with those further out in the plastic zone. The stress field ahead of the crack tip is a function of the radial distance from the tip for a given crack tip velocity. As a result of work hardening, the dislocation density obtained from equation (14) and the dislocation velocity from equation (17) also reach the highest values in the process zone irrespective of their values elsewhere in the plastic zone. If the dislocation velocity in the process zone is independent of the crack tip velocity, the strain rate within the process zone remains constant and therefore, the frictional stress also does not increase.

Figure 7 shows the changes in temperature, dislocation density and the plastic work dissipation rate as function of loading time for the three loading rate parameters considered earlier , however, with the same value of β =10. In contrast to the results shown in Figure 6, obtained at higher crack velocities, the rate of temperature rise in the plastic zone becomes higher along with a similar behavior for the dislocation density and plastic work dissipation rate. Thus, if the alloy microstructure is such that higher loading rates can be attained without increasing the dislocation velocity at the crack tip process zone, higher rates of temperature increase can be expected with an accompanying higher area density of molten regions on the fracture surface. If the dislocation velocity does not increase, the strain rate and the lattice frictional stress also do not increase. Thus, the dislocation density and plastic work rate increase. These results illustrate the importance of the strain rate dependent lattice frictional stress in the crack tip process zone on the changes in temperature.

Influence of Dislocation Velocity

The dislocation velocity at the crack tip is not known precisely in terms of the applied stress and the frictional stress in the lattice. Therefore, we have varied the parameter β by several orders of magnitude keeping the loading rate and crack tip velocity constant. The results obtained for the temperature, and the plastic work dissipation rate near the crack tip are shown in Figure 8. The maximum value of the dislocation density ahead of the crack tip has been found to remain very close for the two values of β with its value continuing to increase after

$t - 10 \times 10^{-4}$ for $\beta = 10$. Therefore, the results of dislocation density are not shown in Figure 7. An increase in dislocation velocity for the same crack tip speed leads to a higher dissipation rate of plastic work and therefore higher temperatures are attained in the process zone. A comparison with the results obtained for an increase in dislocation velocity with a simultaneous increase in crack tip velocity (Figure 5) shows that lower rates of temperature rise are obtained when the crack advances into a region of lower temperature with a higher velocity. Thus, the build up of temperature in the process zone becomes higher only when the crack tip advances to a region within which heat is conducted at a higher rate.

Influence of Lattice Frictional Stress

The lattice frictional stress for the generation and movement of dislocations in the plastic zone is also not known accurately. The previous results are based on the assumption that the frictional stress is one tenth the value of yield stress at 0.2% strain. However, it is known that dislocation movement in crystalline materials takes place at much lower values than the yield stress giving rise to microplasticity. The frictional stress in the lattice is varied to clarify its effect on crack tip changes. We have changed the magnitude of the frictional stress so that its value goes from a tenth to one half and also from a tenth to the magnitude of the yield stress at 0.2% plastic strain. The variation of frictional stress with strain rate and temperature are kept the same as before so that the results can be compared. The generation of the plastic zone takes place only when the stress field ahead of the crack tip rises above the frictional stress. Higher crack tip stress fields are reached after longer time periods of loading if the loading rates remain the same. Thus, the effect of increasing the magnitude of the yield stress is merely to shift the changes in the various quantities towards the right on time scale, as shown in Figure 9. Further, the rate of the temperature increase after the plastic zone starts to develop, remains almost at the same level as obtained earlier with a lower magnitude of frictional stress. This result is significant since crack sizes for longer periods of time will be larger for the same crack velocity and, assuming failure of the specimen begins at a given crack size, the net temperature rise will be smaller at higher frictional stress values.

Influence of Crack Tip Radius

In the present analysis, the crack tip radius, δ, is used to avoid the singularity in the stress field associated with the elastic crack tip. The temperatures attained in the plastic zone are a function of the value of δ. When $\delta = 0$, the crack is perfectly elastic and no plastic zone is formed to give any temperature change.

The crack tip radius depends on the shape and size of the plastic zone into which lattice dislocations move after having been generated at the tip. These lattice dislocations are responsible for rounding the crack tip from an atomically sharp crack at the start. Crack tip blunting depends on the work hardening behavior of the material in the plastic zone. Whereas the effects of the formation of the plastic zone on the crack tip stress field and the resultant changes in temperature will be presented subsequently[58], a simple way to simulate the effects of the crack tip radius is merely to change the magnitude of δ so that the crack tip stress field is altered. This does not include the effect of shift in the crack tip singularity when a plastic zone forms[7] which is important to consider. The results of increasing the crack tip radius by changing δ are shown in Figure 10. It is seen that the rate of temperature rise at the crack tip becomes lower with increasing δ since the magnitude of the crack tip stress and hence the dislocation density and the dissipation rate of plastic work are reduced. Thus, we expect the rate of the temperature increase to be reduced when the material in the process zone becomes more plastic with a lower work hardening coefficient. Thus the model's result of very high crack tip temperatures may be expected only in high strength materials with a high work hardening coefficient and smaller crack tip blunting as a result of the formation of the process zone.

Influence of Distance Moved by Dislocations

Hitherto, we have assumed that the dislocations in the process zone move by a distance equal to the average spacing between dislocations, i.e. $\rho^{-\frac{1}{2}}$. However, if a group of dislocations move simultaneously, the distance moved by the dislocations could be larger. We have calculated the resultant changes in temperature and plastic work rate when the dislocations move larger distances, for example by $10 \cdot \rho^{-1/2}$. The results presented in Figure 11 illustrate that higher temperatures are reached as a result of larger values of plastic work rate, $\dot{W}$.

SUMMARY AND CONCLUSIONS

The energy changes associated with the fast propagation of elastic and plastic cracks have been modeled using crystal plasticity theory with special emphasis on the crack tip region. Dislocation generation rate and dislocation velocity were employed as key parameters in modeling the process zone within the classical plastic zone. The plastic work dissipated at the crack tip was found to result in very high temperature increases for high strength titanium alloys and the influence of the essential parameters on temperature was determined.

Calculations have shown quantitatively for cracks moving at velocities between 0.4 m/s and 1.6 m/s:

1. How the crack tip stress field changes with increasing loading time; and
2. How with increasing distance from the tip
   - (i) the lattice frictional stress increases
   - (ii) the dislocation density increases
   - (iii) the increment of plastic work per unit time increases
   - (iv) the plastic strain increases with each unit of time
   - (v) the dislocation velocity in the plastic zone changes.
3. Temperature changes ahead of the tip as a function of position from the start of crack tip propagation.
4. Relationships between the maximum temperatures attained and
   - (i) the rate of dissipation of plastic work; and
   - (ii) the dislocation density as function of different loading rates, crack tip velocities and dislocation velocities.

A number of general conclusions follow from the numerical results. It is assumed generally that higher loading rates and crack growth velocities will give rise to higher temperatures ahead of the crack tip. However, if the velocity of a very fast crack exceeds the rate of heat conduction the final temperature rise will be lower than that produced at a lower crack velocity. Similarly, a lower crack velocity for which the rate of dissipation of plastic work is low coupled with high thermal conductivity can also lead to low rates of temperature rise. We conclude that there exists a critical crack velocity as a function of thermal conductivity, and the rate of dissipation of plastic work in the process zone for which the build up of temperature becomes most efficient so that the highest temperature is attained. Increasing the crack tip velocity without raising the strain rate dependent lattice frictional stress can also lead to higher temperatures since the plastic zone will form more extensively. The microstructure associated with the region ahead of the crack tip process zone can alter these parameters. Changes in dislocation densities present in the process zone by an order of magnitude can alter the rate of increase of temperature in a given material for a given microstructure. Changing the microstructure can alter the dislocation density and the velocity leading to a different temperature change. The presence of obstacles to dislocation movement in the lattice reduces the dislocation velocity for the same crack tip velocity. In such materials, the frictional stress does not increase with increasing crack tip speed. We have found that the rate of increase of temperature is higher at higher crack growth rates provided the dislocation velocity is kept constant.

ACKNOWLEDGMENTS

This research was supported by the U. S. Office of Naval Research (Grant N00014-82-K-0309) and we wish to thank Dr. Bruce MacDonald for his continuous interest and many stimulating discussions. One of the authors (H.G.F.W.) acknowledges the award of a travel grant from the NATO Scientific Affairs Division, Brussels, Belgium.

References

1. C. Zener and J. H. Hollomon, J. Appl. Phys., 15 (1944) 22-32.
2. J. G. Williams, Applied Materials Research, 4 (1965) 104-106.
3. A. H. Priest, Proc. Int. Conf. on Dynamic Fracture Toughness, Welding Inst., ASM, Metals Park, OH (1977) 95-111.
4. J. M. Krafft and G. R. Irwin, Symposium on Fracture Toughness Testing, STP 381, 114-129, ASTM (1965).
5. I. J. Gruntfest, Fracture of Solids, 189-193, Interscience, New York (1962).
6. J. R. Rice and N. Levy, In Physics of Strength and Plasticity, Ed. A. S. Argon, MIT Press, Cambridge, MA (1969), 277-293.
7. J. R. Rice, Fracture, Ed. H. Liebowitz, Vol. 2, 191-311, Academic Press, New York (1968).
8. B. A. Bilby and J. D. Eshelby, Fracture, Ed. H. Liebowitz, Vol. 1, 99-182, Academic Press, New York (1968).
9. C. Atkinson and M. F. Kanninen, Int. J. Fract., 13, 151-163 (1977).
10. G. T. Hahn, M. F. Kanninen and A. R. Rosenfield, Ann. Review of Materials Science, 2, 381-404 (1972).
11. J. D. Campbell, Mat. Sci. Eng., 12, 3 (1973).
12. J. Eftis and J. M. Krafft, J. Basic Eng., 87, 257-263 (1965).
13. H. D. Kunze and L. W. Meyer, In Metallurgical Applications of Shock Wave and High Strain Rate Phenomena, Eds. L. E. Murr, K. P. Staudhammer and M. A. Meyers, Marcel and Decker Inc., N. Y., 481-507 (1986).
14. J. D. Bryant, D. D. Makel and H. G. F. Wilsdorf, Mat. Sci. Eng., 77, 85-93 (1986).
15. A. J. Rosakis and A. T. Zehnder, In Dynamic Fracture, 169-186, Ed. M. L. Williams and W. G. Knauss, Martinus Nijhoff Publishers, 1985.
16. K. Jagannadham, H. D. Kunze, L. W. Meyer and H. G. F. Wilsdorf, Proc. ICSMA8, Eds. P. O. Kattonen, K. T. Lepisto and M. E. Lehtonen, Pergamon Press, New York (1988) 1095-1100.
17. J. D. Bryant, D. D. Makel and H. G. F. Wilsdorf, In Metallurgical Applications of Shock Wave and High Strain Rate Phenomena, Ed. L. E. Murr, K. P. Staudhammer and M. A. Meyer, M. Dekker, New York (1986) 723-739.
18. C. A. Berg, J. Research of NBS, 76 (1972) 33-39.
19. K. B. Broberg, Fundamentals of Deformation and Fracture, IUTAM, Cambridge University Press, Cambridge, U. K. (1984) 233-242.
20. K. B. Broberg, High Velocity Deformation of Solids, Ed. K. Kawata and J. Shiori, Springer, Berlin (1979) 182-194.
21. F. A. McClintock, Metallurgical Effects at High Strain Rates, Ed. R. W. Rhode, B. M. Butcher, J. R. Holland, and C. H. Karnes, The Metallurgical Society, Plenum Press, New York (1973) 415-423.
22. J. D. Bryant, Deformation Heating at the Crack Tip and its Role in Fracture of Ti-10V-2Fe-3Al, Ph.D. Thesis, Univ. Virginia (1987).
23. D. D. Makel, Strain Rate Dependent Processes in the Fracture of Ti-8Mn, Ph. D. Thesis, Univ. Virginia (1987).
24. H. G. F. Wilsdorf, Acta Metall., 30 (1982) 1247-1258.
25. H. G. F. Wilsdorf, ZS Metallkd. 75 (1984) 154-160.
26. H. G. F. Wilsdorf, Scripta Metall. 17 (1983) 1209-1212.

27. E. Orowan, Proc. Phys. Soc., 52 (1940) 8-22.
28. T. Nicholas, Exp. Mech., 180 (1981) 177.
29. P. S. Follansbee, G. Regazzoni and U. F. Kocks, In Mechanical Properties at High Rates of Strain, Ed. J. Harding, Inst. of Physics, London (1984) 71-80.
30. K. Jagannadham and M. J. Marcinkowski, Unified Theory of Fracture, Ed. F. H. Wohlbier, Trans Tech S.A., Ch-4711 Aedermannsdorf, Switzerland (1983).
31. J. D. Achenbach and M. F. Kanninen, Fracture Mechanics, Ed. N. Perrone, H. Liebowitz, D. Mulville and W. Pilkey, University of Virginia Press (1978) 649-670.
32. R. W. Armstrong, C. S. Coffey and W. L. Elban, Acta Metall., 30 (1982) 2111-2116.
33. R. N. Gardner, T. C. Pollock, and H. G. F. Wilsdorf, Mat. Sci. Eng. 29 (1977) 169-174.
34. T. Vreeland and K. M. Jassby, In Metallurgical Effects at High Strain Rates, Ed. R. W. Rhode, B. M. Butcher, J. R. Holland and C. H. Karnes, The Metallurgical Society, Plenum Press, New York (1973) 277-285.
35. V. I. Alshits and V. I. Indenbom, In Dislocations in Solids,Ed. F. R. N. Nabarro, North Holland, New York (1986), Vol, 7, 46-111.
36. P. A. Mataga, L. B. Freund and J. W. Hutchinson, J. Phys. Chem. Solids, 48 (1987) 985-1005.
37. P. Gillis and J. Kelley, Metallurgical Effects at High Strain Rates, Ed. R. W. Rhode, B. M. Butcher, J. R. Holland and C. H. Karnes, The Metallurgical Society, New York (1973) 287-310.
38. A. V. Granato, Fundamentals of Deformation and Fracture, IUTAM, Cambridge University Press (1984) 188-201.
39. J. P. Hirth and J. Lothe, Theory of Dislocations, McGraw Hill, New York (1968).
40. J. Lothe, J. Appl. Phys., 33 (1962) 2116-2125.
41. C. S. Smith, Trans. AIME, 212 (1958) 574-589.
42. E. Hornbogen, Acta Metall., 10 (1960) 978-980.
43. M. A. Meyers, Scripta Metall., 12 (1978) 21-26.
44. L. E. Murr and D. Kuhlmann-Wilsdorf, Acta Metall., 26 (1978) 847-857.
45. H. Kressel and N. Brown, J. Appl. Phys., 38 (1967) 1618-1625.
46. L. Trieb, J. Appl. Phys., 40 (1979) 2976-2987.
47. F. Seitz and T. A. Read, J. Appl. Phys., 12 (1941) 470-486.
48. J. M. Krafft, Appl. Mater. Res. 3, 88 (1964).
49. D. Kuhlmann-Wilsdorf, Work Hardening in Tension and Fatigue, Ed. A. W. Thompson, AIME (1977) 1-43.
50. A. W. Thompson, Met. Trans., 8A (1977) 833-838.
51. K. B. Broberg, Arkiv Fysik, 18 (1960) 159-192.
52. F. Erdogan, Fracture, Ed. H. Liebowitz, Vol. 2 (1968) 498-590.
53. H. S. Carlslaw and J. C. Jaeger, Conduction of Heat in Solids, Oxford:Clarendon Press (1948) 224-230.
54. A. S. Korhonen and H. J. Kleemola, Met. Trans., 9A (1978) 979-986.
55. Aerospace Structural Metals Hdb., Vol. 2, Code 3707,1-15, Syracuse Univ. Press, New York (1963).
56. J. G. Malcor and F. Montheillet, Deformation of Multi-Phase and Particle Containing Materials, Eds. J. B. Bilde-Sorensen, N. Hansen, H. Horsewell, T. Leffers, and H. Lilholt, Riso, Roskilde, Denmark

57. B.-O. Reinders and H. G. F. Wilsdorf, to be published.
58. K. Jagannadham and H. G. F. Wilsdorf, to be published.

APPENDIX

Notation

G:	Shear Modulus (MPa)
K_{Ic}:	Fracture Toughness (MPa $\sqrt{m}$)
$\dot{K}$:	Loading rate (MPa/s)
V_c:	Crack tip velocity (m/s)
E:	Energy Term (ergs)
E':	Gradient of energy term with crack size (ergs/cm)
$F(V_c)$:	A function of crack tip velocity, V_c; shear wave velocity, c_s; and the dilatational velocity, C_d.
$\dot{W}$:	Rate of plastic work dissipated.
K:	Thermal conductivity (watts/meter °C)
D:	Density (Kg/m^3
C:	Specific heat (J/Kg°C)
F:	Drag force (MPa m)
B:	Drag coefficient (MPa.s)
B_o:	Drag coefficient at absolute zero (MPa.s)
c_s:	Shear wave velocity (m/s)
$T(x_1 t)$:	Temperature as a function of position and time (s)
V:	Dislocation velocity (m/s)
b:	Burger vector of dislocations(m)
d:	Average distance moved by the dislocation (m)
r:	Radial distance from the tip (m)
h:	Grid spacing in the plastic zone for finite difference equation (m
t:	Loading time (s)
a:	Thermal diffusivity (K/DC)

k: Boltzmanns Constant (ergs/^{o}K)

α: a constant (0.5)

σ: Crack tip stress field (MPa)

σ_{yy}: Component of crack tip stress field (MPa)

σ_{a}: Applied stress (MPa)

σ_{o}: Lattice frictional stress (MPa)

σ_{y}: Yield stres at 0.2% strain (MPa)

τ: Resolved shear stress on a dislocation (MPa)

$\dot{\varepsilon}$: Strain rate (s^{-1})

ϕ: Geometric factor

ρ: Dislocation density (m^{-2})

ρ_{m}: Mobile dislocation density (m^{-2})

$\dot{\rho}$: Dislocation generation rate (m^{-2} s^{-1})

λ: Lifetime of a dislocation (s)

β: Parameter used for changing dislocation velocity as a function of applied stress

h: $V_{c}\Delta t$ (m)

ν: Poisson's ratio

δ: Region within which elastic stress field becomes invalid (used to represent crack tip radius) (m)

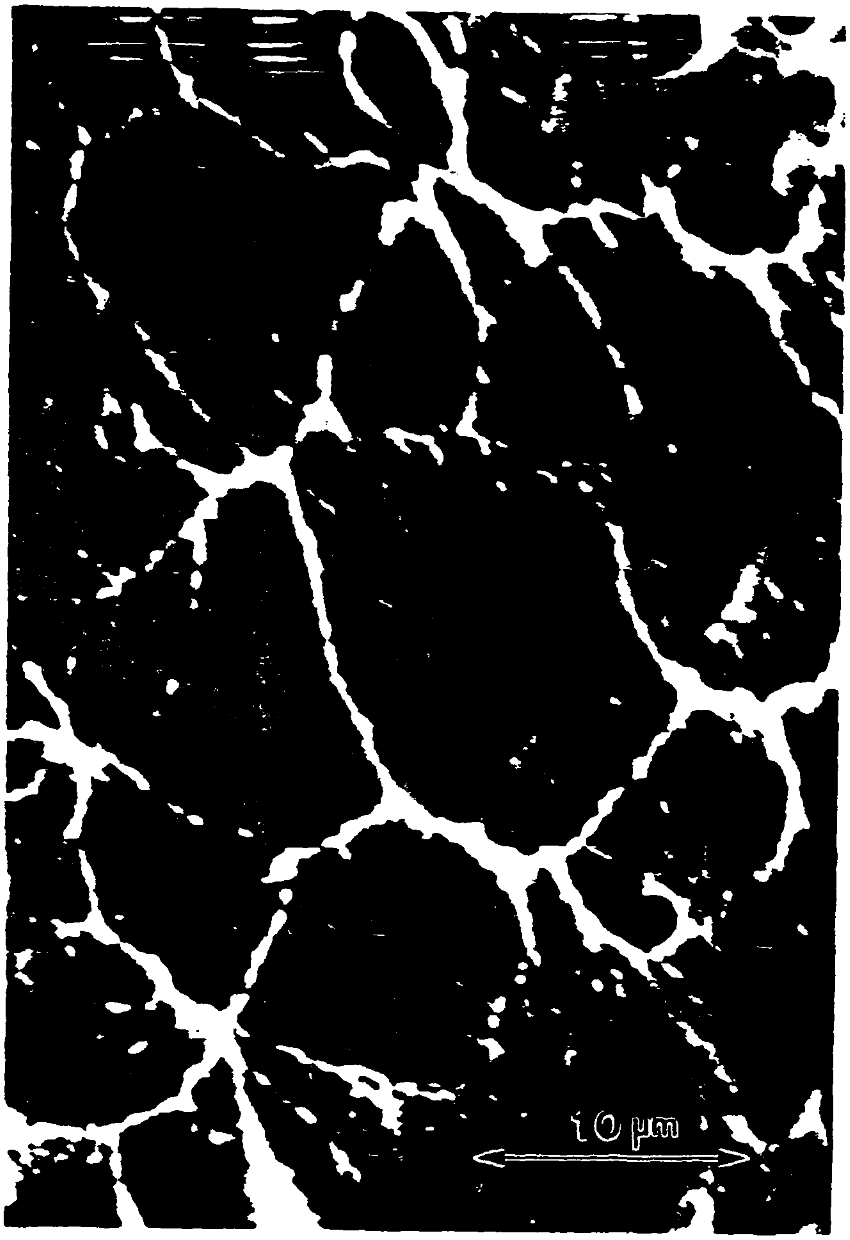

Fig. 1. Scanning electron micrograph of a fracture surface of Ti-10V-2Fe-3Al showing a solidified droplet-like structure at the rim of dimples. Also note particles at the bottom of dimples which are not present on normal fracture surfaces.

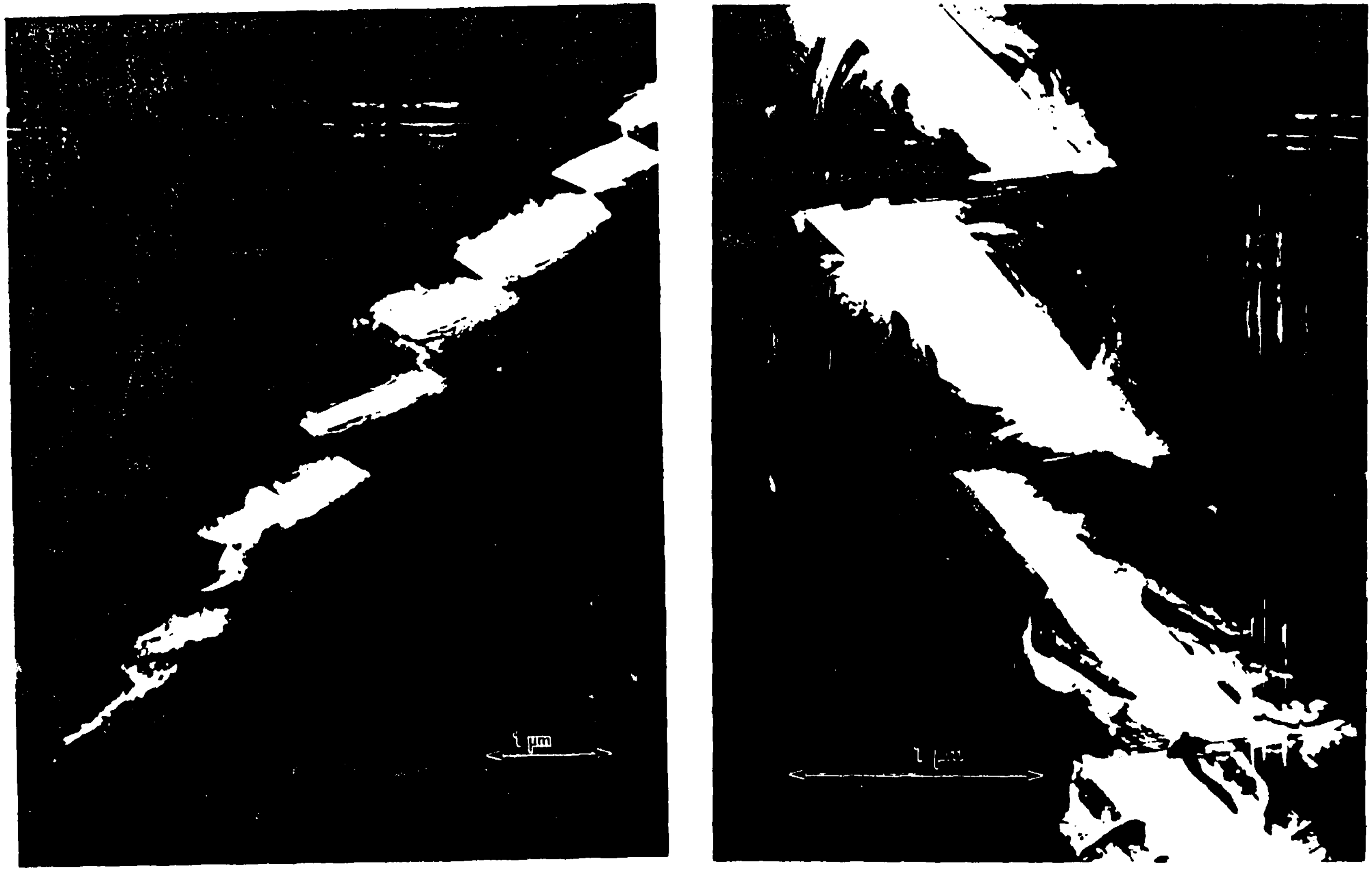

Fig. 2(a). Transmission electron micrograph obtained by <u>in-situ</u> straining to fracture of a gold foil. Crack opens up via many holes with microligaments between holes. (b) Microligaments rupture along $\bar{1}10$ and shear parallel to 112 . Glide processes have been explained earlier in gold[24] and other metals and alloys[25].

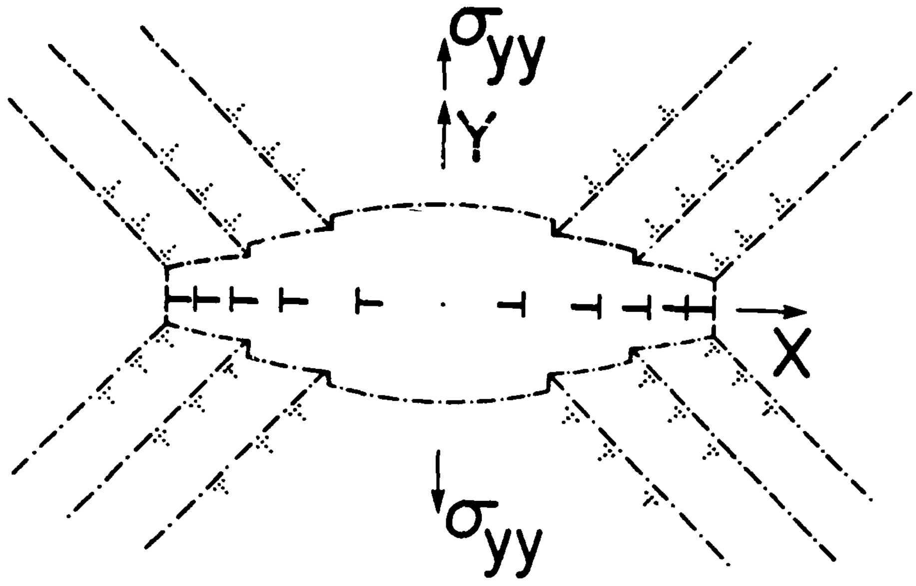

Fig. 3. Schematic illustration of the dislocation description of a continuous plastic crack. The dislocations shown in full line are crack dislocations and those shown dotted are lattice dislocations.

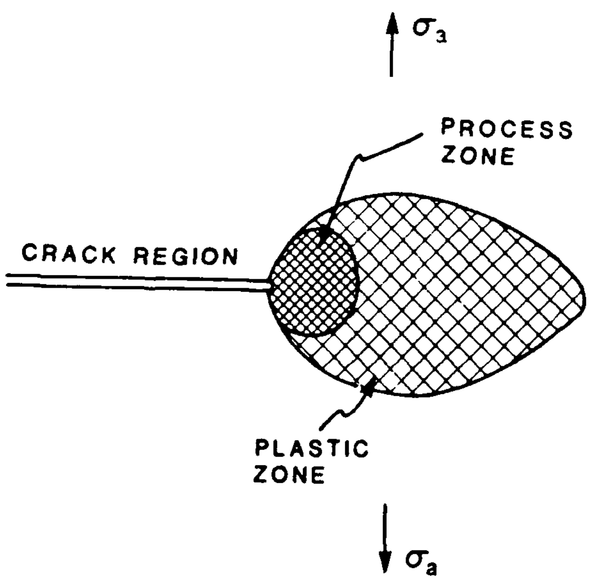

Fig. 4. A schematic illustration of a crack subjected to a uniform applied tensile stress with the plastic zone and the process zone formed at the tip. The process zone is identified by the high density of dislocations. The transition from the process zone to the plastic zone is gradual.

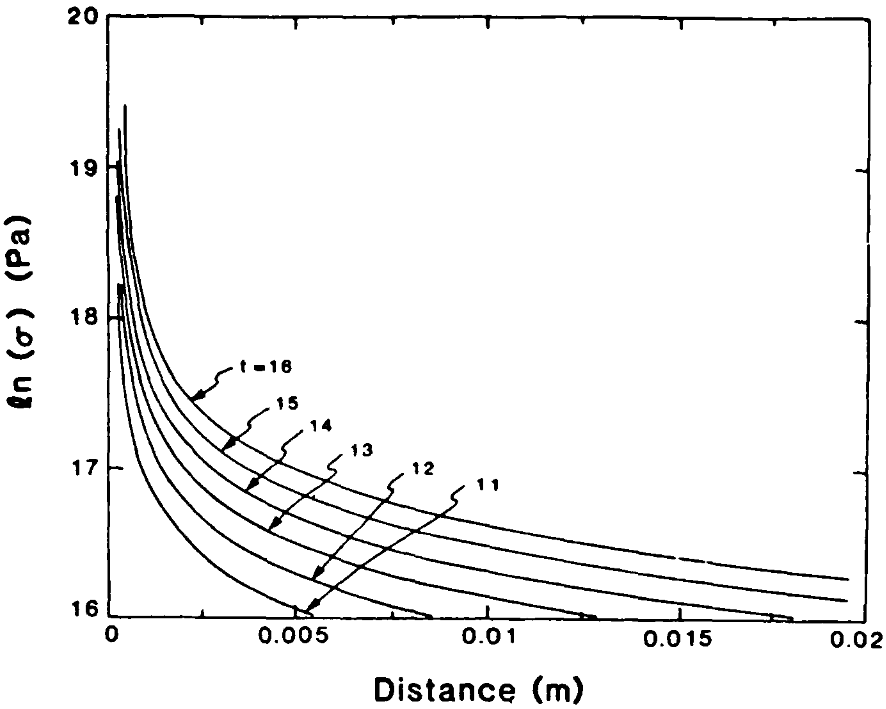

Fig. 5(a) The stress field ahead of the crack tip given by equation (15) shown as a function of the position from the starting point of the crack. The loading rate $\dot{K}$ = 680 MPa/sec and the crack tip velocity V_c = 0.4 meter/sec. The parameter β = 10 has been chosen to determine the dislocation velocity from equation (17). The lattice frictional stress is chosen at one tenth the value of the yield stress at 0.2% strain. The stress levels are shown for different values of time t in units of 10^{-4} seconds.

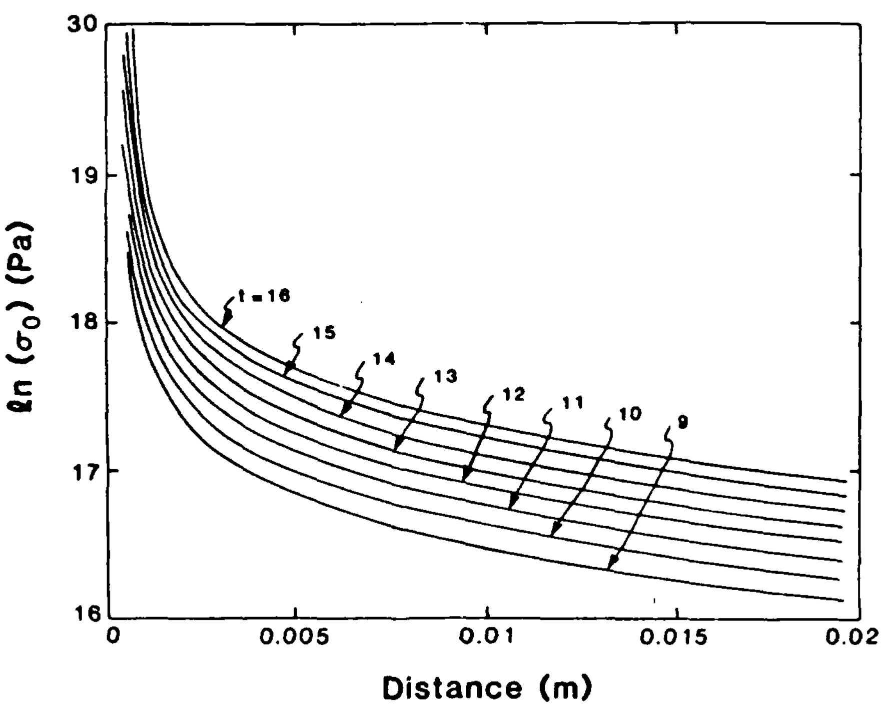

Fig. 5(b) Same as Figure 5(a) but the strain rate dependent lattice frictional stress has been shown as a function of position from the start.

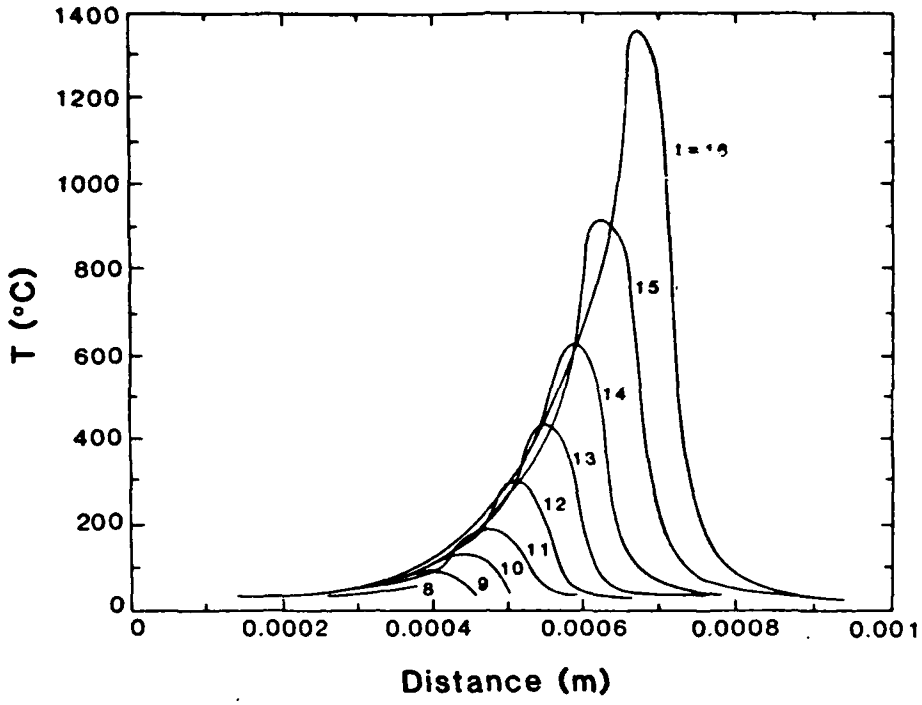

Fig. 5(c) Same as Figure 5(a) but the temperature ahead of the crack tip is shown as a function of position from the start.

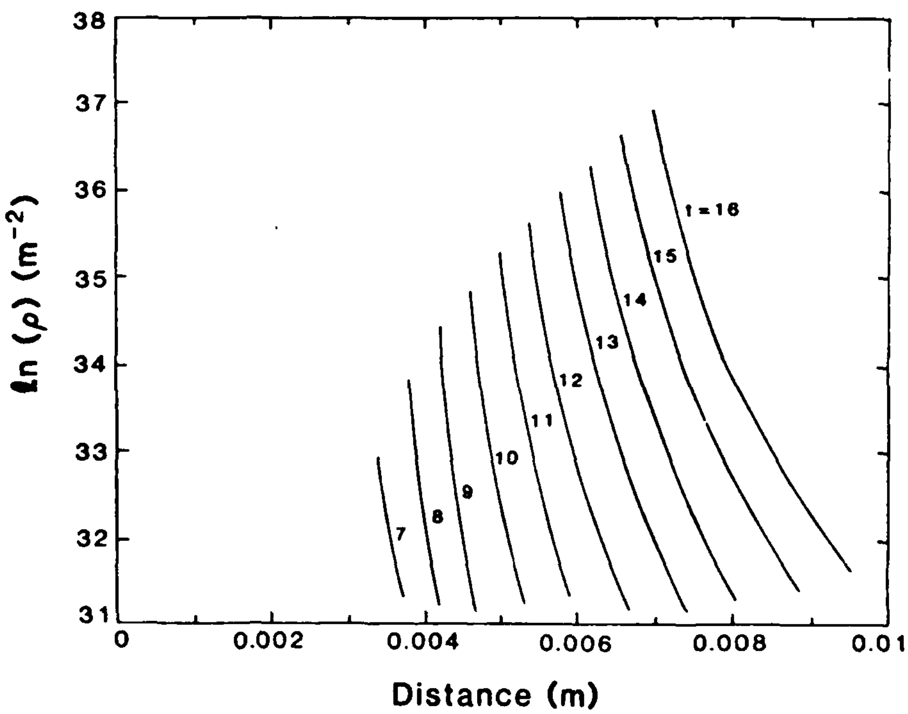

Fig. 5(d).Same as Figure 5(a) but the dislocation density is shown as a function of position. Each curve represents the decrease in dislocation density from its maximum value at the crack tip.

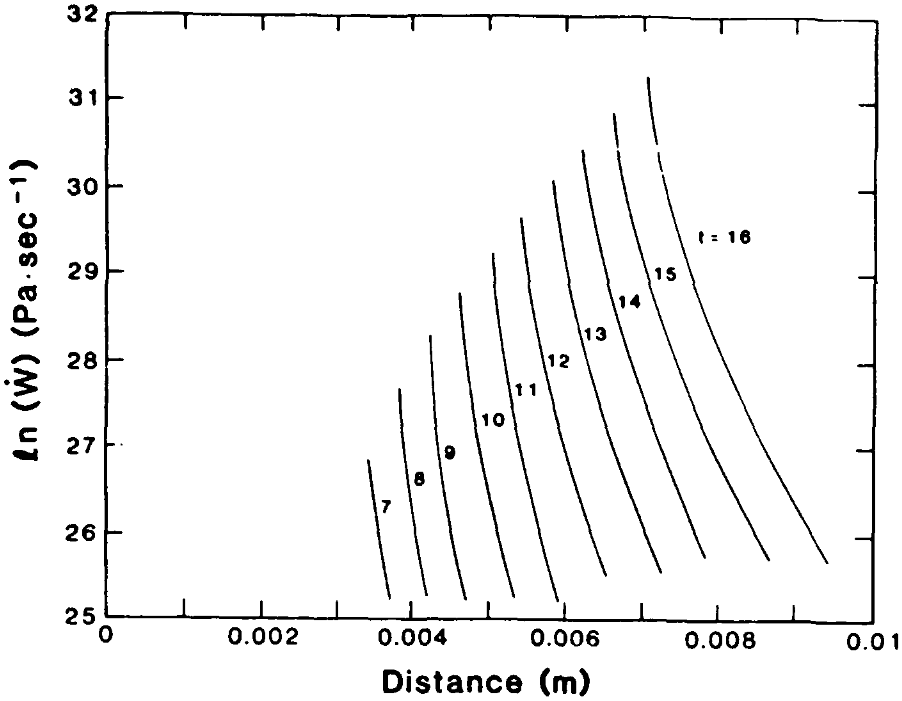

Fig. 5(e) Same as Fig. 5(a) but the plastic work dissipated per unit time is shown as a function of position from the maximum at the crack tip.

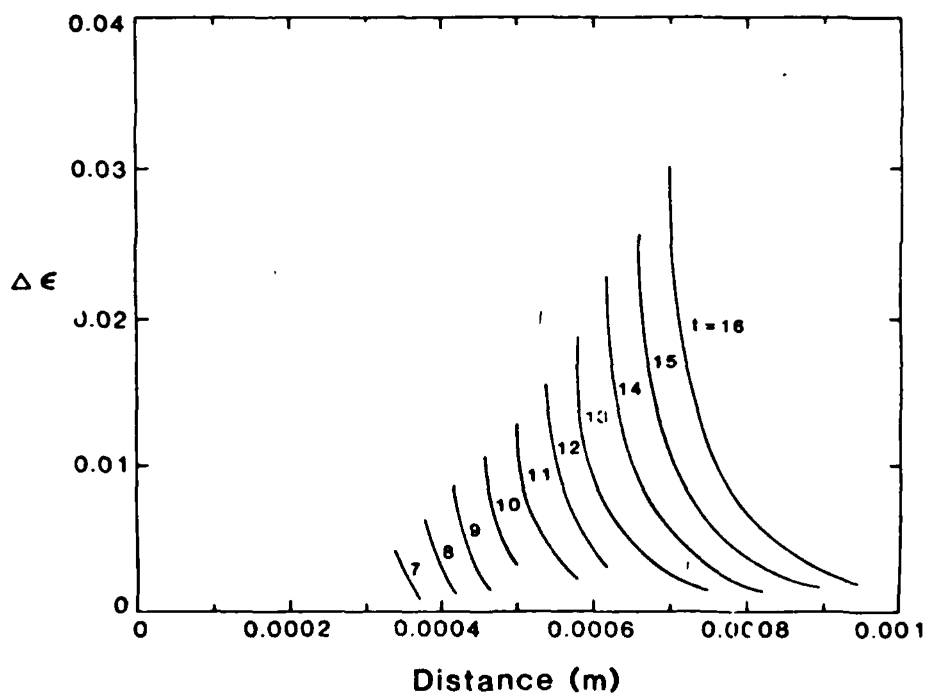

Fig. 5(f) Same as Fig. 5(a) but the increment of plastic strain ahead of the crack tip is shown as a function of position from the maximum at the crack tip.

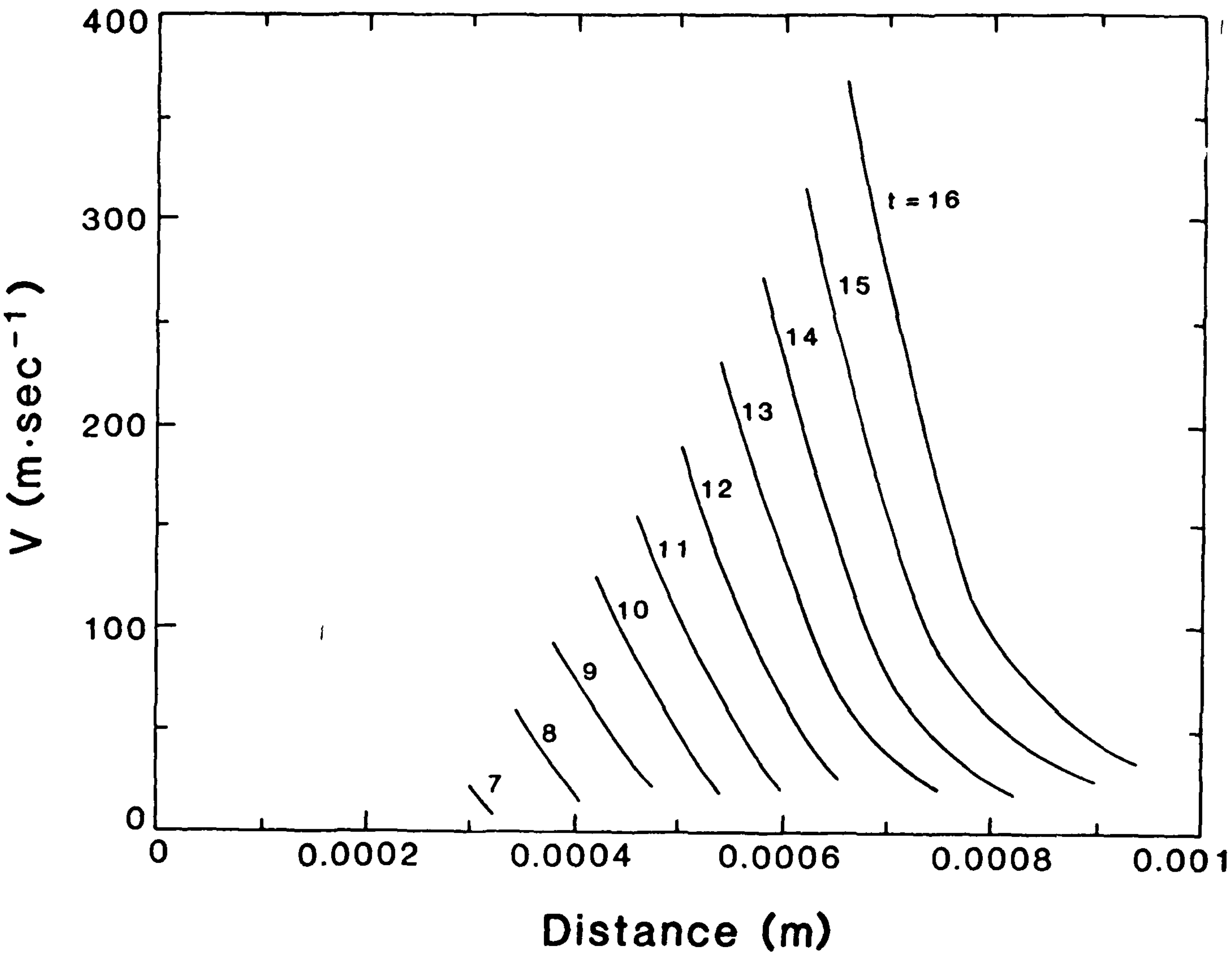

Fig. 5(g) Same as Figure 5(a) but the dislocation velocity V, ahead of the crack tip in the plastic zone is shown as a function of position from the maximum at the crack tip.

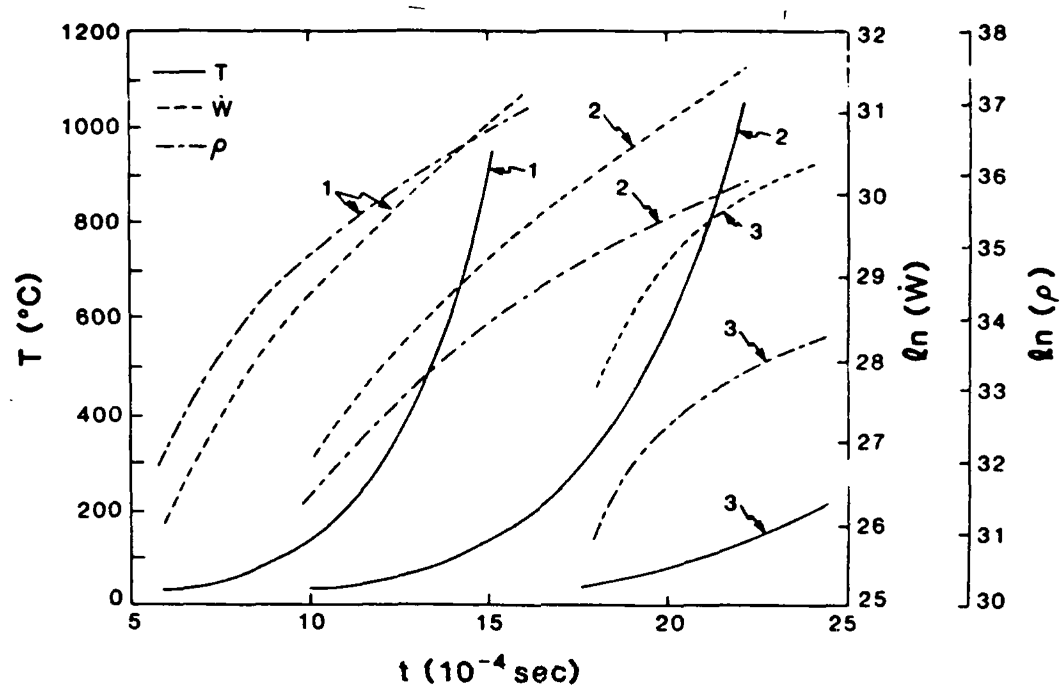

Fig. 6. The maximum temperature attained in the plastic zone ahead of the crack tip, the rate of dissipation of plastic work, Ẇ, and the dislocation density, shown as a function of loading time for three different conditions:

(1) $\dot{K}$ = 680 MPa/sec, $\sigma_o = \sigma_y/10$, V_c = 0.4 m/sec and β = 10

(2) $\dot{K}$ = 888 MPa/sec, $\sigma_o = \sigma_y/10$, V_c = 0.8 m/sec and β = 20,

(3) $\dot{K}$ = 1160 MPa/sec, $\sigma_o = \sigma_y/10$, V_c = 1.6 m/sec and β = 40.

The value of β has been increased by the same factor as that of V_c so that the macroscopic strain rate is proportional to the loading rate.

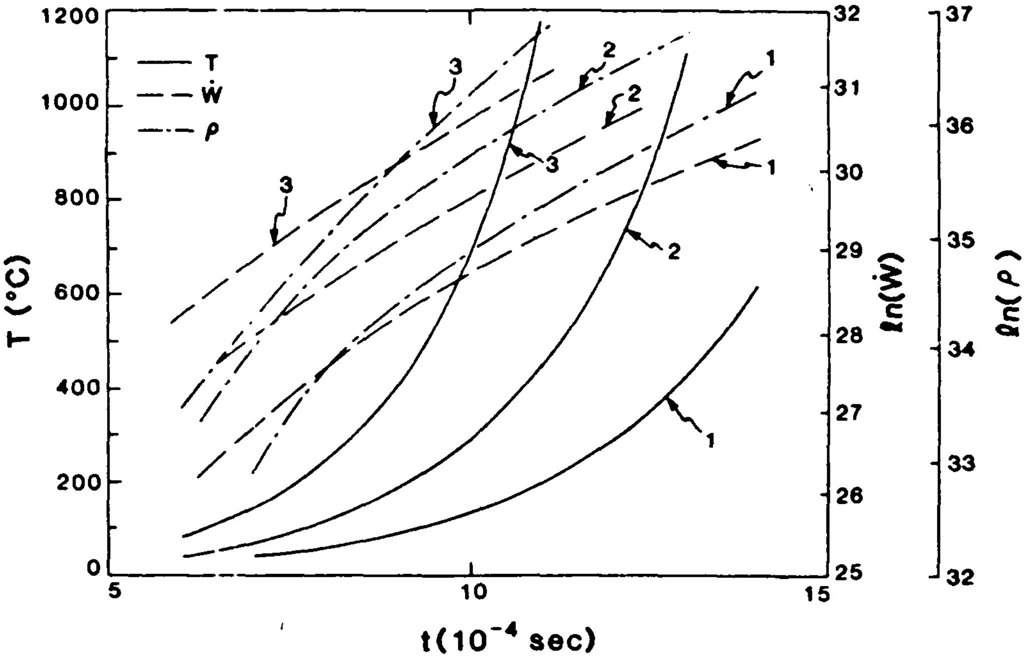

Fig. 7. The maximum temperature attained in the plastic zone ahead of the crack tip, the rate of dissipation of plastic work, $\dot{W}$ and the dislocation density, ρ, shown as a function of loading time for three different conditions:

(1) $\dot{K}$ = 680 MPa/sec, $\sigma_o = \sigma_y/10$, V_c = 0.4 m/sec and ß = 10

(2) $\dot{K}$ = 888 MPa/sec, $\sigma_o = \sigma_y/10$, V_c = 0.8 m/sec and ß = 10

(3) $\dot{K}$ = 1160 MPa/sec, $\sigma_o = \sigma_y/10$, V_c = 1.6 met/sec and ß = 10

The value of ß has been kept constant for all values of the loading rate, $\dot{K}$, and crack tip velocity, V_c so that the dislocation velocity and the strain rate near the crack tip are independent of the macroscopic strain rate.

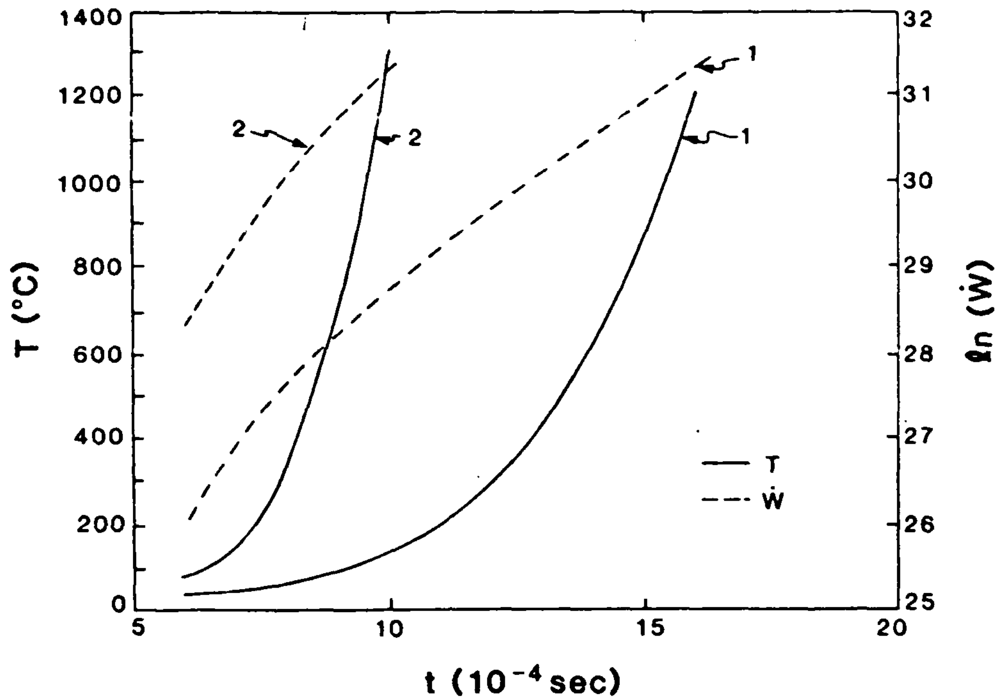

Fig. 8. The maximum temperature T attained in the plastic zone ahead of the crack tip, the rate of dissipation of plastic work, $\dot{W}$, shown as a function of loading time t for two different conditions: $\dot{K}$ = 680 MPa/sec, $\sigma_o = \sigma_y/10$, V_c = 0.4 m/sec, and (1) β = 10, (2) β = 100. These results illustrate the the influence of dislocation velocity ahead of the crack tip for constant values of $\dot{K}$, V_c and σ_o. The dislocation density in the plastic zone remains the same for the two values of β up to t = 10 x 10^{-4} and increases further for β = 10, therefore, the dislocation density has not been shown in this figure.

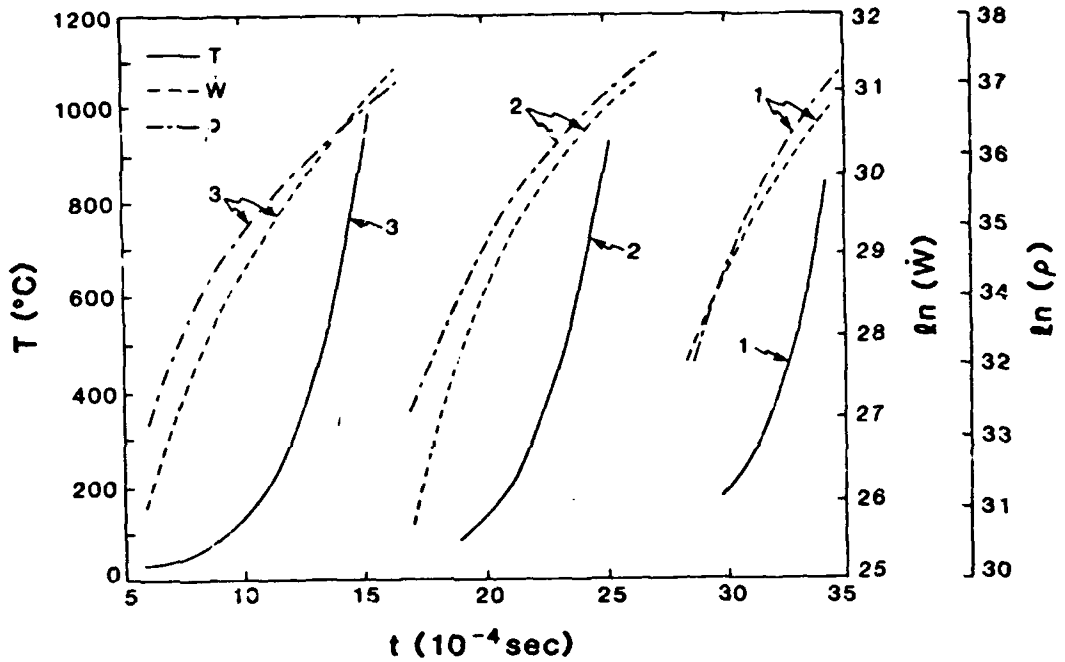

Fig. 9. The maximum temperature T attained in the plastic zone ahead of the crack tip, the rate of dissipation of plastic work, $\dot{W}$, and the dislocation density, ρ, shown as a function of loading time for three different conditions: $\dot{K}$ = 680 MPa/sec, V_c = 0.4 m/sec, β = 10, with (1) $\sigma_o = \sigma_y$, (2) $\sigma_o = \sigma_y/2$, and (3) $\sigma_o = \sigma_y/10$. These results illustrate the influence of frictional stress in the lattice.

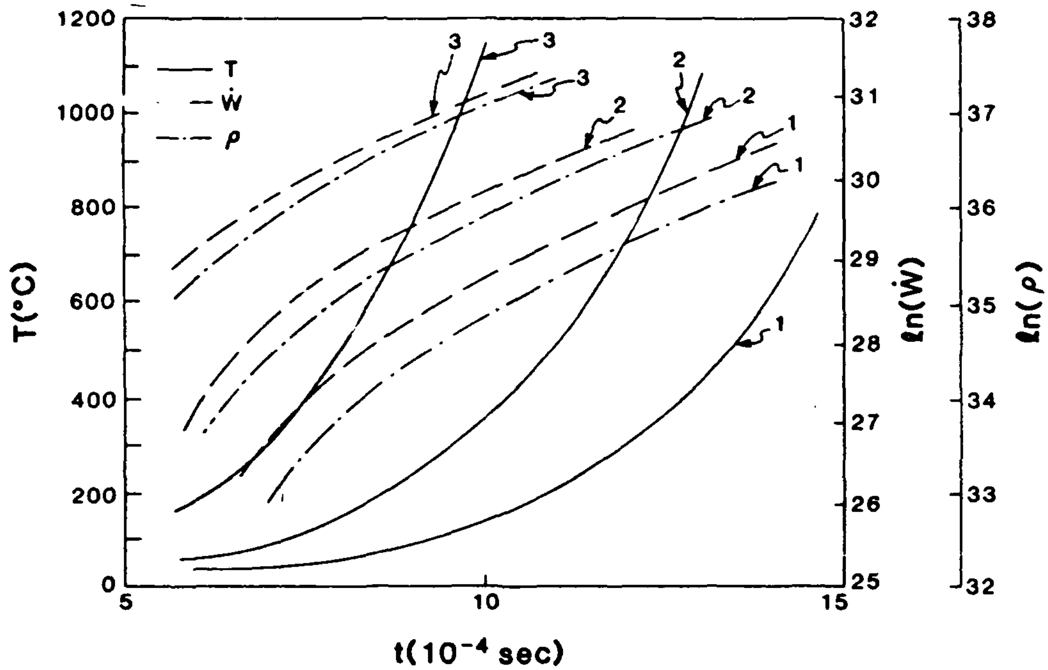

Fig. 10. The maximum temperature attained within the plastic zone ahead of the crack tip, the rate of dissipation of plastic work, $\dot{W}$ and the dislocation density, ρ, shown as a function of loading time for three different conditions: $\dot{K}$ = 680 MPa/sec, β = 10, $\sigma_o = \sigma_y/10$, V_c = 0.4 m/sec and (1) $\delta = 0.5V_c\,\Delta t$, (2) $\delta = 0.25V_c\,\Delta t$, (3) $\delta = 0.1V_c\,\Delta t$. These results illustrate the effect of the crack tip radius.

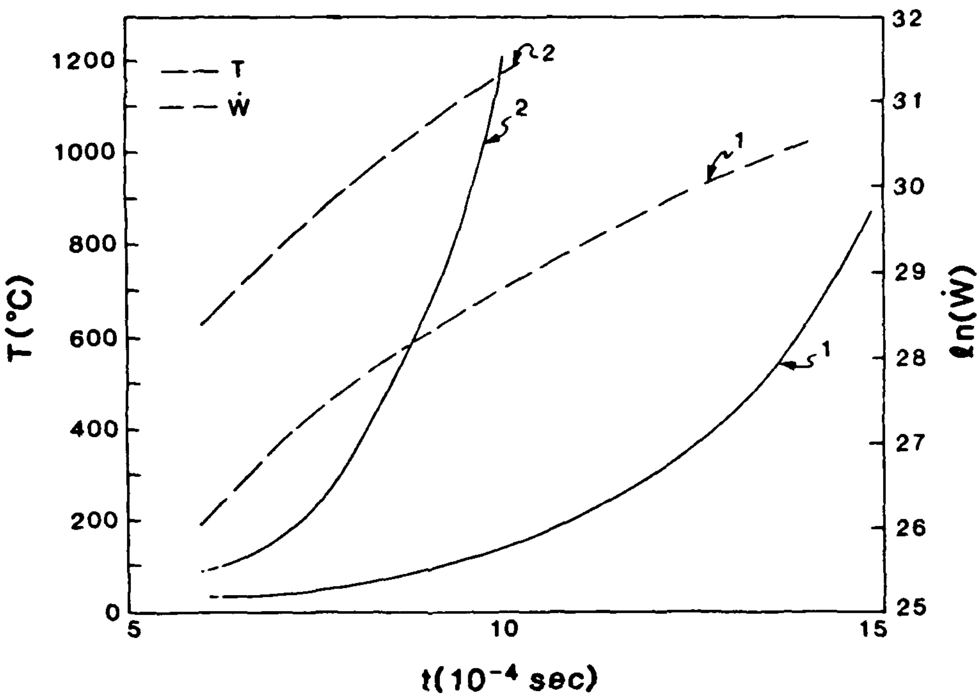

Fig. 11. The maximum temperature attained within the plastic zone ahead of the crack tip, the rate of dissipation of plastic work, $\dot{W}$, shown as a function of loading time for two different conditions; $\dot{K}$ = 680 MPa/sec, V_c = 0.4 m/sec, $\beta = 10$, $\sigma_o = \sigma_y/10$, with (1) $d = (\rho)^{-\frac{1}{2}}$, and (2) $d = 10(\rho)^{-\frac{1}{2}}$. These results illustrate the effect of distance travelled by dislocation ahead of the crack tip in comparison to the average distance between dislocations.